Chinese Chemical Letters 35 (2024) 109135

Contents lists available at ScienceDirect

Chinese Chemical Letters

journal homepage: www.elsevier.com/locate/cclet

Removal of Microcystin-LR in lake water sample by hydrophilic mesoporous silica composites under high-throughput MALDI-TOF MS detection platform

Wantong Zhang[a], Zixing Xu[a], Guofei Dai[c,*], Zhijian Li[b,*], Chunhui Deng[a,*]

[a] Department of Chemistry, Institute of Metabolism & Integrate Biology (IMIB), Fudan University, Shanghai 200433, China
[b] Jiangxi Key Laboratory of Organic Chemistry, Jiangxi Science and Technology Normal University, Nanchang 330013, China
[c] Jiangxi Academy of Water Science and Engineering, Nanchang 330029, China

ARTICLE INFO

Article history:
Received 20 May 2023
Revised 6 September 2023
Accepted 18 September 2023
Available online 22 September 2023

Keywords:
Microcystin-LR
Mesoporous silica
Magnetic composites
MALDI-TOF MS analysis

ABSTRACT

Microcystins (MCs), a family of cyclic heptapeptide cyanotoxins, exists in aquatic environment where cyanobacterial bloom happens, which will accumulate in aquatic organisms and transfer through the food chain to higher trophic levels, posing a health risk to both animals and human bodies. Among various MCs, Microcystin-LR (MC-LR) is worthiest studied for its strong toxicity, ubiquity and widespread. Here in this work, iminodiacetic acid (IDA) decorated magnetic mesoporous silica ($mSiO_2$) nanocomposites (Fe_3O_4@$mSiO_2$-IDA) were facilely synthesized which possessed the merits of large surface area (188.21 m^2/g), accessible porosity (2.66 nm), excellent hydrophilicity and rapid responsiveness to magnetic field. Then the composites were successfully employed to the removal process of Microcystin-LR in real water samples followed by Matrix-assisted laser desorption/ionization time-of-flight mass spectrometry (MALDI-TOF MS) analysis, achieving the removal efficiency above 92.5% even after ten recycles of the composites. It provided a potential method for removing MC-LR in aqueous environment with high effectiveness, lower costs and less secondary contamination.

Cyanobacterial bloom is one of the most common phenomenon of water pollution which occurs because of the mass propagation of Cyanobacteria and is influenced dominantly by temperature, light and nutrients in the aquatic environment [1]. The significant production of secondary metabolites which are defined as cyanotoxins is secreted by various blue-green algae. Those cyanotoxins can accumulate in aquatic organisms and transfer through the food chain to higher trophic levels, posing a health risk to both animals and human bodies [2,3]. Among all kinds of cyanotoxins, Microcystins (MCs) are frequently studied owing to their high toxic [4] and diversity [5]. It has been reported that MCs is a family of biologically active cyclic heptapeptide cyanotoxins consisting a general cyclo-(D-Ala1-X2-D-MeAsp3-Z4-Adda5-D-Glu6-Mdha7) structure with more than 80 variants [6,7], in which X and Z position is occupied by variable L-amino acids. The microcystin-LR (MC-LR), with the L-leucine and L-arginine amino acids substitute on X and Z respectively, has universally been used as research subject for its strong toxicity, ubiquity and abundance [8,9]. Considering the risks brought to human health by MCs, the World Health Organization (WHO) recommends a guideline that the total concentration of MCs in drinking water should be controlled below 1 μg/L [10]. Furthermore, the unique cyclic structure and amino acids contribute to the good water solubility and heat resistance, allowing them stably present in aquatic environment with different pH values for several months and years [11]. Therefore, removing MC-LR in an effective and rapid manner is essential to protect the ecological environment.

To date, many methods from physical, biological and chemical fields have been developed to remove MC-LR in water solutions. However, owing to the high stability attributed to the chemical structure of MC-LR, boiling and other conventional water treatment process cannot remove MC-LR completely [12,13]. Moreover, traditional treatments including membrane filtration, ultrasound, chemical oxidation and biological enzymes have obvious drawbacks such as high cost, low economic effect and secondary contamination [14–18]. Nowadays, various adsorption treatment are attractive alternatives to MC-LR removal and has received considerable attention [19–22]. Ideal adsorption-based strategies such as Magnetic solid-phase extraction (MSPE), Metal oxide affinity chromatography (MOAC) and Immobilized metal affinity chromatog-

* Corresponding authors.
E-mail addresses: daiguofei@whu.edu.cn (G. Dai), lizhijianhdd@163.com (Z. Li), chdeng@fudan.edu.cn (C. Deng).

https://doi.org/10.1016/j.cclet.2023.109135
1001-8417/

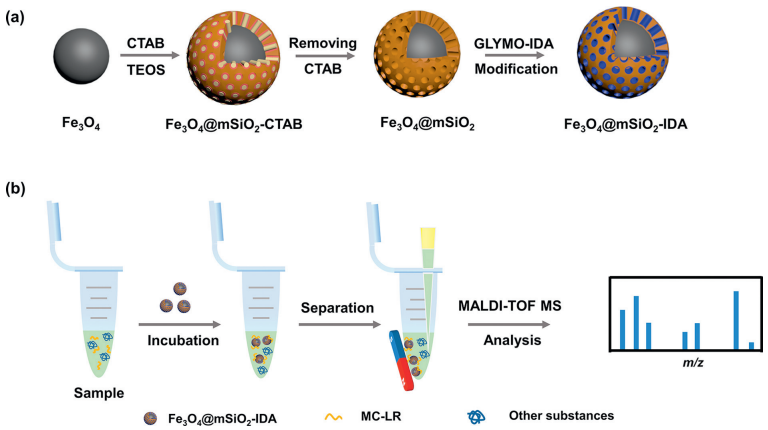

Scheme 1. (a) The synthetic route of Fe_3O_4@SiO_2-IDA composites. (b) The workflow of the removal process.

raphy (IMAC) are more potential for MC-LR removal in practical application in rapid separation and recycle from real lake environment comparing with commonly used Capillary microextraction (CME) strategy [23], especially the utilization of magnetic nanocomposites [24–31]. Comparing with commonly used porous solid absorbent activated carbon [32,33], mesoporous magnetic nanocomposites are pore-size controllable and easy to recycle from solution. Recently, mesoporous carbon materials and carbon functionalized mesoporous silica materials have been conclusively investigated. The unique structure of mesopores can provide large surface area and abundant adsorption sites for MC-LR adsorption.

Various analysis techniques have been employed for detecting the MC-LR in aqueous solution, including liquid chromatography/mass spectrometry (LC/MS) [34], high-performance liquid chromatography (HPLC) [35]. These frequently used analytical methods have been comprehensively developed which are mature technology. Nevertheless, LC/MS and HPLC take long time for analysis. Matrix-assisted laser desorption/ionization time-of-flight mass spectrometry (MALDI-TOF MS), as a quick and rapid responsive technique, possessing the ability to identify individual toxin substances, has been successfully applied in the analysis of MCs [36]. Hence, it is feasible to combine removal process with MALDI-TOF MS analysis to design a simple and efficient method for removing MC-LR in water samples.

In this work, hydrophilic magnetic mesoporous silica materials defined as Fe_3O_4@mSiO$_2$-IDA was designed and synthesized, constructing by magnetic Fe_3O_4 core and evenly mesoporous SiO_2 channels shell (mSiO$_2$) with iminodiacetic acid (IDA) grafted. The Fe_3O_4@mSiO$_2$-IDA composites were characterized to measure the mesoporous structure as well as confirm the successful immobilization of IDA by using silane coupling agent (3-glycidoxypropyldimethoxymethylsilane, GLYMO). Except for combining the merits of magnetic nanocomposites and mesoporous silica materials, it also possessed greater hydrophilicity which enhanced by zwitterionic group imported from IDA [37]. According to previous study, MC-LR, as a special type of N-linked peptide, can strongly interact with hydrophilic groups provided by IDA. Meanwhile, suitable mesopore diameters provided by mesoporous silica are beneficial to MC-LR adsorption *via* pore diffusion [38]. Thus, Fe_3O_4@mSiO$_2$-IDA composites were adopted to the removal of Microcystin-LR in aqueous solution for the first time and achieved great results. MALDI-TOF MS analysis technique was introduced to directly detect the relative concentration of MC-LR in water sample rapidly and sensitively. The removal condition was explored, and the adsorption characteristics of nanomaterials had been investigated. Finally, the developed removal process was applied in real lake water sample collected from Poyang Lake, suggesting that Fe_3O_4@mSiO$_2$-IDA composites have significant potential of removal treatment in MC-LR contaminated water.

The synthetic route of Fe_3O_4@SiO_2-IDA composites is presented in Scheme 1a**.** Firstly, GLYMO-IDA solution was prepared by reacting silane coupling reagent (GLYMO) with IDA under 65 °C water bath for 4 h. Secondly, the Fe_3O_4 nanoparticles were synthesized through a hydrothermal reaction. Next, tetraethyl orthosilicate (TEOS) was employed as a source of silica to coat a layer of mesoporous silica onto the surface of Fe_3O_4 with the assistant of structure-directing agent (cetyltrimethylammonium bromide, CTAB). Finally, the Fe_3O_4@mSiO$_2$-IDA was obtained by grafting prepared GLYMO-IDA solution into the formed mesoporous channels.

The Fe_3O_4@mSiO$_2$ and Fe_3O_4@mSiO$_2$-IDA composites were characterized by transmission electron microscope (TEM) to evaluate the mesoporous and core-shell structures of the as prepared materials and the morphology of them was investigated by field emission scanning electron microscope (FESEM). As shown in Fig. 1, both Fe_3O_4@mSiO$_2$ and Fe_3O_4@mSiO$_2$-IDA possess a homogeneous spherical morphology with clear mesoporous silica cladding layer, while Fe_3O_4@mSiO$_2$-IDA has a rougher surface. Comparing with Fe_3O_4@mSiO$_2$ composites with a 39 nm thick thickness mesoporous silica layer, it can be clearly observed that Fe_3O_4@mSiO$_2$-IDA maintains a sequentially arranged mesoporous structure and the average thickness of coating layer has increased to 44 nm after decorated by GLYMO-IDA solution. The dynamic light scattering (DLS) characterization (Figs. S1b and c in Supporting information) confirms the increasement of particle size as well. In addition, the TEM images display well-separated Fe_3O_4 nanoparticles which could be attributed to the coating of mesoporous silica, indicating the great prevention of spontaneous aggregation of magnetic particles. The results of element mapping of Fe_3O_4@mSiO$_2$-IDA in Fig. 1e manifests the existence of Fe, Si, O, C and N, illustrating the existence of IDA groups**.** The porosity characteristics of Fe_3O_4@mSiO$_2$ and Fe_3O_4@mSiO$_2$-IDA composites were measured by nitrogen adsorption-desorption isotherms at 77 K. Fig. 1f and Fig. S1a (Supporting information) both exhibited a typical IV isotherm with a small hysteresis loop which represents the mesoporous property of Fe_3O_4@mSiO$_2$ and Fe_3O_4@mSiO$_2$-IDA composites, respectively. The BET surface area and pore volume of Fe_3O_4@mSiO$_2$-IDA composites were calculated to be 188.21 m^2/g and 0.151 cm^3/g, respectively. The considerably large surface area provided by Fe_3O_4@mSiO$_2$-IDA composites create an ideal adsorption condition. By Barret-Joyner-Halenda (BJH) method, the pore size distribution map (inset in Fig. 1f and Fig. S1 in Supporting information) was obtained with the results which shows the pore width of Fe_3O_4@mSiO$_2$-IDA was 2.66 nm, while the pore width

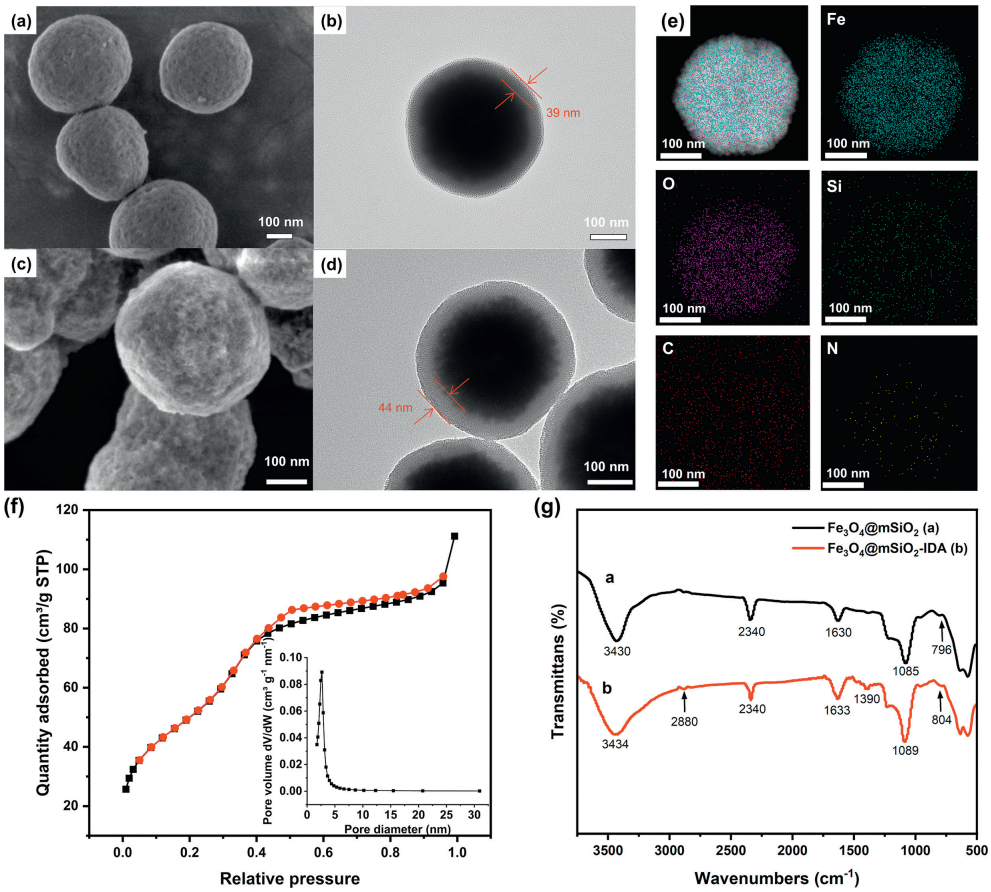

Fig. 1. FESEM images of Fe_3O_4@mSiO_2 (a) and Fe_3O_4@mSiO_2-IDA (c). TEM images of Fe_3O_4@mSiO_2 (b) and Fe_3O_4@mSiO_2-IDA (d). (e) Element mapping of Fe_3O_4@mSiO_2-IDA. (f) The nitrogen adsorption-desorption isotherms of Fe_3O_4@mSiO_2-IDA composites. (g) FT-IR spectra of Fe_3O_4@mSiO_2 and Fe_3O_4@mSiO_2-IDA.

of Fe_3O_4@mSiO_2 was 3.10 nm. The reported universal diameter of MC-LR is smaller than 2 nm [39], which means the Fe_3O_4@mSiO_2-IDA has a more suitable mesoporous channels for MC-LR to get access.

To verify the successful modification of IDA, FT-IR spectroscopy was portrayed for Fe_3O_4@mSiO_2 and Fe_3O_4@mSiO_2-IDA (Fig. 1g), in which both curves own the band at 796-804 cm^{-1} is attribute to the symmetric vibration of Si-O-Si, and the adsorption peaks at 1085-1089 cm^{-1} is assigned to the asymmetric stretching vibration of Si-O-Si. This illustrated the silica has successfully coated on the surface of Fe_3O_4 nanoparticles [40]. The emerging adsorption peak at 2880 cm^{-1} which can be ascribed to the CH_2 stretching vibration appeared after the decoration of GLYMO-IDA solution. Moreover, the presence of the adsorption band at 1390 cm^{-1} is considered to be CH_2-N units [41]. Moreover, the EDX element analysis (Fig. S2 in Supporting information) revealed the carbon and nitrogen content on the surface of Fe_3O_4@mSiO_2-IDA drastically increased. Comparing Fe_3O_4@mSiO_2 with the iron and silica content has decreased. Additionally, the zeta potential of Fe_3O_4, Fe_3O_4@mSiO_2 and Fe_3O_4@mSiO_2-IDA are 21.9, −19.8, and −36.8 mV, respectively (Fig. S3a in Supporting information). It can be obviously observed that the zeta potential turns to negative from positive after coating mesoporous silica and showing a more negative potential after the modification of GLYMO-IDA. All these above results confirm the existence of IDA on Fe_3O_4@mSiO_2 surface and the successful synthesis of Fe_3O_4@mSiO_2-IDA composites.

The magnetic properties of Fe_3O_4@mSiO_2-IDA were displayed in Fig. S3b (Supporting information), which demonstrates excellent magnetism. The hydrophilicity of Fe_3O_4@mSiO_2 and Fe_3O_4@mSiO_2-IDA were determined by water contact angle analysis. The water contact angles of Fe_3O_4@mSiO_2 and Fe_3O_4@mSiO_2-IDA were 26.33° and 20.55°, respectively (Fig. S3c in Supporting information). The results indicated both two composites have an excellent hydrophilicity, but Fe_3O_4@mSiO_2-IDA was much more hydrophilic than the former. Furthermore, the Fe_3O_4@mSiO_2-IDA composites were well dispersed in water and can easily aggregate with the presence of extra magnet within 60 s (Fig. S3b), meeting the demand of rapid removal and simple recycling. The results found that mesoporous silica wrapping and IDA decoration on the Fe_3O_4 play a crucial role in hydrophilicity and dispersibility, which is beneficial to MC-LR adsorption in water.

Fe_3O_4@mSiO_2-IDA composites possess high surface area, ample adsorption positions, excellent hydrophilicity and magnetism, making it an ideal removal material to remove poisonous MC-LR quickly and environmentally friendly. Scheme 1b illustrates the workflow of the removal process. Firstly, 150 μg materials were directly added into 100 μL 10 μg/L MC-LR standard aqueous solution and incubated at 37 °C for 20 min. The incubation process allows materials adequately contact with MC-LR and capture them into its mesoporous structure. Next, an extra magnet was introduced to separate materials from solution. Then the supernatant was collected for MALDI-TOF MS analysis. The mass spectra of standard 10 μg/L MC-LR aqueous solution and the collected supernatant removed by Fe_3O_4@mSiO_2-IDA were displayed in Fig. 2a. The intensity of MC-LR before and after the removal process were 1802 a.u. and 125 a.u., resulting a removal efficiency of 93.3%. Comparing with the removal efficiency attained by adopting Fe_3O_4@mSiO_2, Fe_3O_4@mSiO_2-IDA achieved a higher removal effect because the modification by GLYMO-IDA improves the hydrophilicity of Fe_3O_4@mSiO_2 (Fig. 2b). These re-

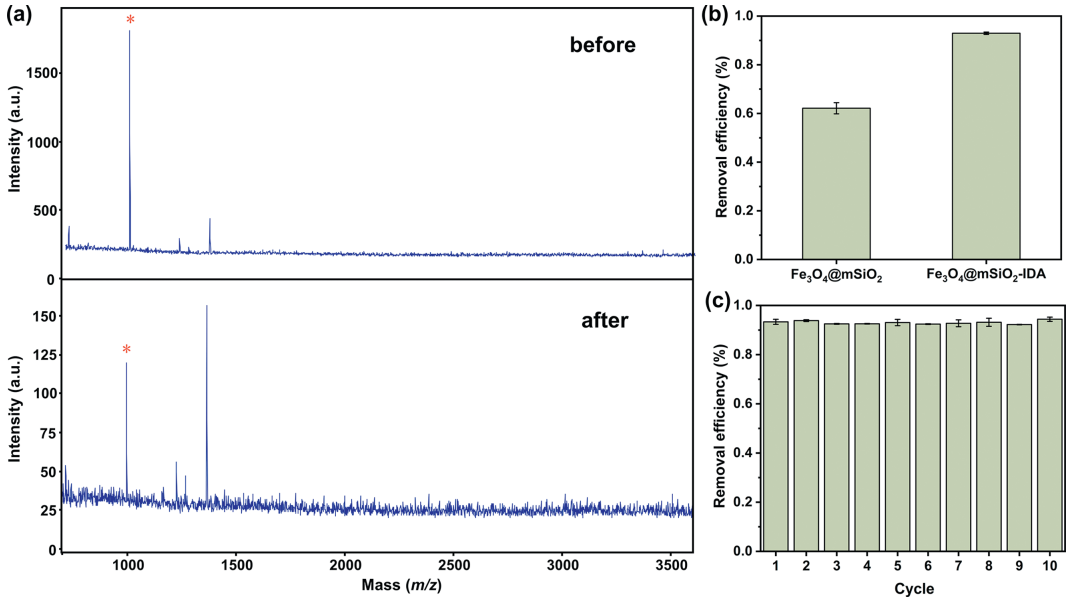

Fig. 2. (a) The mass spectra of 10 μg/L MC-LR aqueous solution before and after the removal process by using Fe_3O_4@$mSiO_2$-IDA composites. (b) Comparison of removal efficiency by using Fe_3O_4@$mSiO_2$ and Fe_3O_4@$mSiO_2$-IDA in 10 μg/L MC-LR standard aqueous solution. (c) Regeneration study of Fe_3O_4@$mSiO_2$-IDA composites by using 50% ACN/0.1% TFA for continuous cycles.

sults show that the significant effectivity and prominent removal performance of Fe_3O_4@$mSiO_2$-IDA in removing MC-LR in aquatic environment.

In order to gain the best removal efficiency, the optimal removal conditions were evaluated from different amounts of removal materials, removal time and temperature on the removal process. In this section, 100 μL 10 μg/L MC-LR standard aqueous solution was selected to simulate the real water environment.

25-300 μg Fe_3O_4@$mSiO_2$-IDA were designed to investigate the optimal amount of removal materials. From Fig. S4a (Supporting information), the removal efficiency drastically increased when the amount of removal materials increasing from 0 to 100 μg and then reached equilibrium at 150 μg. Thus, 150 μg Fe_3O_4@$mSiO_2$-IDA was adopted in later study. It also noted that Fe_3O_4@$mSiO_2$-IDA possess sufficient adsorption sites and strong interaction with MC-LR, which allows high removal efficient can be achieved by using a small quantity of removal materials.

The removal time is considered to be an important indicator to examine the removal efficiency. Therefore, the study was conducted by incubating Fe_3O_4@$mSiO_2$-IDA with MC-LR standard aqueous solution within 0-40 min. Fig. S4b (Supporting information) clearly shows the removal efficiency reached maximum at about 30 min, which can attribute to the excellent dispersion of Fe_3O_4@$mSiO_2$-IDA in water and the strong interaction between removal materials and MC-LR. Therefore, the Fe_3O_4@$mSiO_2$-IDA can rapidly remove MC-LR in 30 min.

It is indispensable to employ above removal process under different temperatures. Thus, the influence brought by temperature was studied at 15 °C, 25 °C and 37 °C, respectively. The results showed that the removal efficiency remained essentially constant at different temperatures (Fig. S4c in Supporting information), which demonstrate the excellent potential of Fe_3O_4@$mSiO_2$-IDA to remove MC-LR in different external environment.

The adsorption performance of Fe_3O_4@$mSiO_2$-IDA nanocomposites under pH 2-9 was investigated. As shown in Fig. S5a (Supporting information), the removal efficiency reached at an optimal value of 95% at pH 3, 4, and 5, while the removal performance decreased at pH 2 and higher pH. However, throughout the experiment results, the removal efficiency was not dramatically affected with pH varied, suggesting that Fe_3O_4@$mSiO_2$-IDA has significant potential in removing MC-LR from sophisticated aquatic environment with different pH.

Moreover, the *zeta* potential of Fe_3O_4@$mSiO_2$-IDA after adsorbed with MC-LR was obviously different from the unabsorbed one (Fig. S5b in Supporting information), suggesting the existence of electrostatic interaction between Fe_3O_4@$mSiO_2$-IDA and MC-LR. Next, the pH_{PZC} of Fe_3O_4@$mSiO_2$-IDA was experimentally derived to be 5.06 (Fig. S5c in Supporting information), indicating that Fe_3O_4@$mSiO_2$-IDA owned positive charges when the solution pH was below 5.06, otherwise it was negative. According to previous work, MC-LR molecule which possessed one -NH_2 and two -COOH groups, charged differently when pH values varied, such as MC-LR^+ (pH < 2.09), MC-LR^0 (2.09 < pH < 2.19), MC-LR^- (2.19 < pH < 12.48) [42]. The results indicated that Fe_3O_4@$mSiO_2$-IDA carried negative charges had stronger electrostatic interaction with MC-LR^+ at lower pH, contributing the higher removal efficiency at pH 3, 4 and 5. Under the condition of pH 2, the proportion of MC-LR^+ decreased which triggered the increase of electrostatic repulsion between Fe_3O_4@$mSiO_2$-IDA and MC-LR, leading to the lower removal efficiency. Furthermore, the hydrophobic interaction could occur between the Fe_3O_4@$mSiO_2$-IDA and MC-LR owing to the hydrophobic Adda and Leu residues resided on MC-LR [38].

To further know about the mechanism of interactions between Fe_3O_4@$mSiO_2$-IDA and MC-LR, the adsorption kinetics examination was conducted under the optimal conditions in which 150 μg Fe_3O_4@$mSiO_2$-IDA were introduced in 100 μL 10 μg/L MC-LR standard aqueous solution at 37 °C. As shown in Fig. S6 (Supporting information), the adsorption capacities increase rapidly in the initial 0.2 h due to the high MC-LR concentration and adequate adsorption sites on the Fe_3O_4@$mSiO_2$-IDA composites. Then the adsorption rate slows down with the increasing of the time at the 0.2-0.4 h. Ultimately, the adsorption plateaued in the 0.5 h. The Pseudo-first order (PFO), and Pseudo-second order (PSO) adsorption kinetics models were applied to fit the adsorption equilibrium experiment data. It can be seen that the PSO model was better fitted to the kinetic results with higher correlation coefficient ($R^2 = 0.96$), suggesting the chemical interaction was dominant between removal materials and MC-LR.

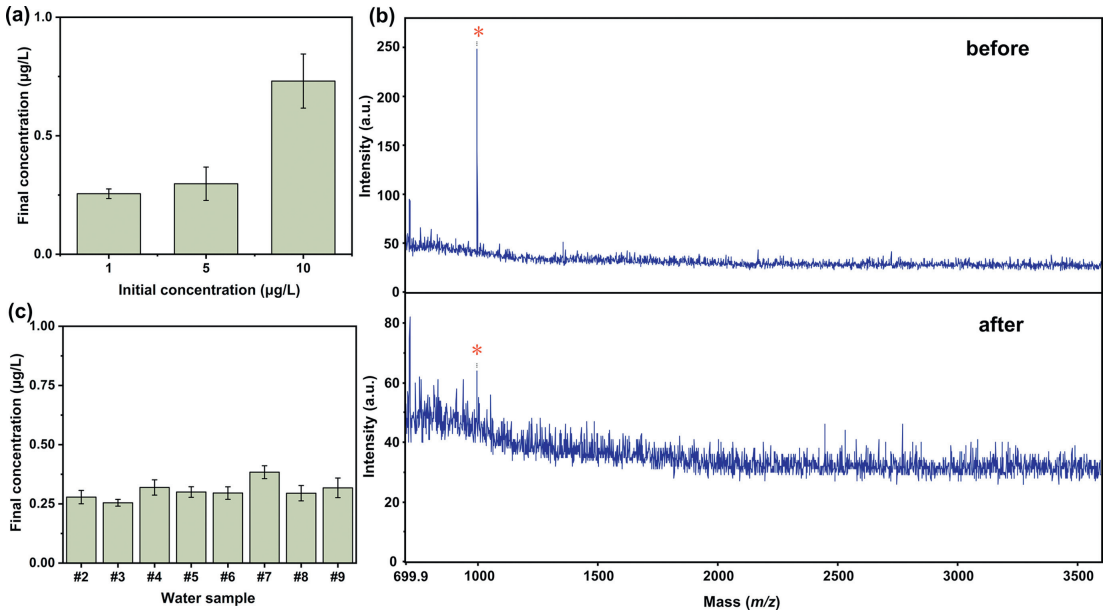

Fig. 3. (a) Removal of MC-LR (1, 5 and 10 μg/L) in #1 real lake water sample collected from Poyang Lake by Fe_3O_4@mSiO_2-IDA composites. (b) Mass spectra of MC-LR (1 μg/L) in #1 real lake water sample before and after removal process. (c) The removal efficiency of 1 μg/L MC-LR in real lake water sample collected from different latitudes and longitudes of Poyang Lake.

Economic factors are also important evaluation criteria for the removal process which is mainly determined by the regeneration efficiency of removal materials. Different from magnetic nanomaterials chelated with metal ions which is difficult to desorb captured MC-LR [43], Fe_3O_4@mSiO_2-IDA can be easily recycled by commonly used eluent. Referred to previous studies, three different eluents (50% ACN/0.1% TFA, 25 mmol/L ammonium bicarbonate solution and 0.4 mol/L ammonium hydroxide) were employed to test the regeneration efficiency for MC-LR. All the removal process was conducted under the same conditions and the Fe_3O_4@mSiO_2-IDA with MC-LR fully absorbed were collected. Then, 10 μL different eluents were added to thoroughly wash off the MC-LR about 30 min and then delivered to MALDI-TOF MS. The mass spectra suggested that 50% ACN/0.1% TFA was the most ideal eluent with highest intensity of MC-LR peak (Fig. S7 in Supporting information). Therefore, 50% ACN/0.1% TFA was employed in the following experiment. In addition, the results demonstrated the existence of hydrogen bond between MC-LR and Fe_3O_4@mSiO_2-IDA according to previous study [44]. The hydrogen bond was formed between -NH_2 and -COOH groups of MC-LR and oxygenic functional groups of Fe_3O_4@mSiO_2-IDA.

The optimal elution time was investigated with the vibration time range of 2-40 min and the results displayed that the MC-LR was completely washed off after 30 min (Fig. S8 in Supporting information). Furthermore, the removal efficiency maintained above 92.5% during 10 cycles of removal-elution process (Fig. 2c), supporting 50% ACN/0.1% TFA could serve as an ideal eluent which has achieved an excellent regeneration efficiency and indicating Fe_3O_4@mSiO_2-IDA is an economic, environmentally friendly, stable and easily recycled removal material.

In order to determine the selectivity of the proposed removal process, the selectivity experiment was conducted by investigating the removal performance of Fe_3O_4@mSiO_2-IDA nanocomposites among various interferents and MC-LR. As shown in Fig. S9 (Supporting information), seven small-molecule dyes with similar molecular weight and size (Table S2 in Supporting information) to MC-LR were employed with removal efficiency all lower than 20%, illustrating the remarkable selectivity of MC-LR by using the Fe_3O_4@mSiO_2-IDA nanocomposites as absorbent. The excellent selectivity can be contributed to the richer -NH_2 and -COOH groups provided by MC-LR to interact with IDA and the electrostatic interaction, hydrogen bond and hydrophobic interaction between Fe_3O_4@mSiO_2-IDA and MC-LR.

The concentration of MC-LR when algal bloom occurs can reach up to 50 μg/L [45]. However, according to the guideline from WHO, human health would under risks when the concentration of MC-LR in aqueous water environment is higher than 1 μg/L. Therefore, in this research, environmentally relevant concentrations (1, 5, and 10 μg/L) of MC-LR were employed to simulate the real algal bloom environment by adding MC-LR standards into real lake sample (Sample #1 in Table S3 in Supporting information) collected from Poyang Lake. After removal by Fe_3O_4@mSiO_2-IDA, the final concentrations of MC-LR were all meet the WHO criteria (Fig. 3a), with mass spectra of MC-LR before and after removal process in Fig. 3b and Fig. S10 (Supporting information).

Referring to previous report, the contamination and water quality varied according to geographic location [46]. Thus, for a comprehensive analysis, water samples were collected from different latitudes and longitudes of Poyang Lake (Table S2) to simulate the process of MC-LR removal. As shown in Fig. 3c, the removal efficiency of 1 μg/L MC-LR in real lake water sample stayed above 64%, and the final concentration of MC-LR were all lower than 1 μg/L, suggesting that Fe_3O_4@mSiO_2-IDA can be universally adopted for the removal of MC-LR from different real water samples. Furthermore, the proposed removal process was in comparison with previous works to investigate the potential practicability in real lake aquatic environment (Table 1) [33,44,47-50]. Comparing with other magnetic nanoparticles, the developed removal process showed remarkable advantages in BET surface area and less pretreatment time. Although Zeng's work achieved greater BET surface area, the pretreatment time is long [33]. Moreover, better than cyclodextrin-modified magnetic nanoparticles G-Fe_2O_3-CD which cyclodextrins detachment occurs during regeneration steps [47], Fe_3O_4@mSiO_2-IDA shows the excellent recovery rate with stable zwitterionic group decoration provided by GLYMO-IDA and less removal time.

In this work, the Fe_3O_4@SiO_2-IDA composites which have large surface area (188.21 m^2/g), accessible porosity (2.66 nm), excellent hydrophilicity and rapid responsiveness to magnetic field were

Table 1
Comparison of the proposed method with previous methods.

Absorbent	BET surface area (m^2/g)	Pretreatment time	Technique	Recycle times	Ref.
Fe_3O_4@PDA@γ-CDP	56.1	37 min	HPLC-MS/MS	3	[48]
Fe_3O_4@SiO_2@P-CDP	50.1	97 min	HPLC-MS/MS	5	[44]
IL@MG	123.64	20 min	UPLC-MS/MS	3	[49]
CPC@SiO_2@Fe_3O_4	–	40 min	HPLC-UV	3	[50]
Fe_3O_4@mSiO_2-IDA	188.21	30 min	MALDI-TOF MS	10	This work
FA-BCs	835.10	2 d	HPLC-C18 column	4	[33]
G-Fe_2O_3-CD	400	2 h	HPLC-UV	<4	[47]

successfully applied in MC-LR removing in aqueous environment with high efficiency and environmental-friendly. The utilization of small amount of Fe_3O_4@SiO_2-IDA composites achieved the removal efficiency above 93.3% and the treated aqueous solution of MC-LR meets the guideline set by WHO (containing MC-LR lower than 1 μg/L). The kinetics study indicated that the MC-LR absorption on the mesoporous structure of Fe_3O_4@SiO_2-IDA occurred by chemical interaction. For economics concerned, regeneration study provided a surprising result with high regeneration efficiency, which achieved the removal efficiency stayed above 92.5% after ten removal-elution cycles. Finally, the designed removal process had successfully employed in real lake water environment, suggesting the Fe_3O_4@SiO_2-IDA composites have significant potential for removing lake water polluted by MC-LR or other hydrophilic contaminants.

Declaration of competing interest

The authors declare that they have no known competing financial interests or personal relationship that could have appeared to influence the work reported in this paper.

Acknowledgments

This work was financially supported by National Key R&D Program of China (No. 2018YFA0507501) and the National Natural Science Foundation of China (Nos. 22074019, 21425518, 22004017, 22205085, and 32160305), Key Science and Technology Project of Jiangxi Province (Nos. 20213AAG01012 and 2022KSG01004), Water Science and Technology Project of Jiangxi Province (Nos. 202124ZDKT19 and 202223YBKT07) and Shanghai Sailing Program (No. 20YF1405300).

Supplementary materials

Supplementary material associated with this article can be found, in the online version, at doi:10.1016/j.cclet.2023.109135.

References

[1] S. Merel, D. Walker, R. Chicana, et al., Environ. Int. 59 (2013) 303–327.
[2] L. Chen, J. Chen, X. Zhang, P. Xie, J. Hazard. Mater. 301 (2016) 381–399.
[3] Y. Li, J. Chen, Q. Zhao, et al., Environ. Health Perspect. 119 (2011) 1483–1488.
[4] D. Feurstein, K. Holst, A. Fischer, D.R. Dietrich, Toxicol. Appl. Pharmacol. 234 (2009) 247–255.
[5] J. Puddick, M.R. Prinsep, S.A. Wood, et al., Mar. Drugs. 12 (2014) 5372–5395.
[6] A. Campos, V. Vasconcelos, Int. J. Mol. Sci. 11 (2010) 268–287.
[7] R.P. Rastogi, R.P. Sinha, A. Incharoensakdi, Rev. Environ. Sci. Biotechnol. 13 (2014) 215–249.
[8] A.I. Prieto, A. Jos, S. Pichardo, et al., Environ. Toxicol. 24 (2009) 563–579.
[9] J. McElhiney, L.A. Lawton, Toxicol. Appl. Pharmacol. 203 (2005) 219–230.
[10] A.A. de la Cruz, M.G. Antoniou, A. Hiskia, et al., Anti-Cancer Agents Med. Chem. 11 (2011) 19–37.
[11] Y. He, P. Wu, G. Li, et al., Int. J. Biol. Macromol. 156 (2020) 1574–1583.
[12] W. Liu, C. Gan, W. Chang, et al., Anal. Chim. Acta 1054 (2019) 128–136.
[13] N. Khadgi, A.R. Upreti, Chemosphere 221 (2019) 441–451.
[14] W. Xu, XX. Li, YP. Li, et al., Environ. Pollut. 291 (2021) 118143.
[15] P. Kumar, HDP. Rubio, K. Hegde, et al., Sci. Total Environ. 670 (2019) 971–981.
[16] M. Crettaz-Minaglia, Environ. Sci. Pollut. Res. 27 (2020) 44427–44439.
[17] P. Kumar, H. Rehab, K. Hegde, et al., Sci. Total Environ. 703 (2020) 135052.
[18] M.J. Sampaio, L.M. Pastrana-Martinez, AM. Silva, et al., RSC Adv. 5 (2015) 58363–58370.
[19] K. Wu, B. Wang, B. Tang, et al., Chin. Chem. Lett. 33 (2022) 2721–2725.
[20] J. Zhong, J. Zhou, M. Xiao, et al., Chin. Chem. Lett. 33 (2022) 973–978.
[21] X. Zhang, Y. Yang, P. Qin, et al., Chin. Chem. Lett. 33 (2022) 903–906.
[22] J. Yang, J. Qin, Z. Guo, Y. Hu, X. Zhang, Chin. Chem. Lett. 32 (2021) 1819–1822.
[23] T. Huang, X. Lei, S. Wang, C. Lin, X. Wu, J. Chromatogr. A 1692 (2023) 463849.
[24] M. Zhan, Y. Hong, Curr. Pollut. Rep. 8 (2022) 113–127.
[25] G. Liu, H. Chen, W. Zhang, et al., Anal. Chim. Acta 1166 (2021) 338539.
[26] S. Liu, Talanta 154 (2016) 183–189.
[27] J. Lu, J. Zhou, H. Guo, et al., J. Chromatogr. A 1676 (2022) 463290.
[28] H. Chen, X. Lu, C. Deng, X. Yan, J. Phys. Chem. C 113 (2009) 21068–21073.
[29] Z. Wang, C. Huang, N. Sun, C. Deng, Sci. China Chem. 64 (2021) 932–947.
[30] Z. Li, Y. Wang, A.A. Elzatahry, et al., Chin. Chem. Lett. 31 (2020) 1598–1602.
[31] J. Li, R. Yao, B. Deng, et al., Chem. Eng. J. 464 (2023) 142626.
[32] H.J. Song, R. Gurav, S.K. Bhatia, et al., J. Water Process Eng. 41 (2021) 102054.
[33] S. Zeng, E. Kan, Chemosphere 273 (2021) 129649.
[34] M.R. Neffling, L. Spoof, J. Meriluoto, Anal. Chim. Acta 653 (2009) 234.
[35] L. Spoof, K. Karlsson, J. Meriluoto, J. Chromatogr. A 909 (2001) 225–236.
[36] H. Liu, X. Lu, C. Deng, X. Yan, Rapid Commun. Mass Spectrom. 27 (2013) 2515–2518.
[37] J.B. Schlenoff, Langmuir 30 (2014) 9625–9636.
[38] J.A. Park, J.K. Kang, S.M. Jung, et al., Chemosphere 247 (2020) 125811.
[39] Z. Svirčev, D. Drobac, N. Tokodi, et al., Arch. Toxicol. 91 (2017) 621–650.
[40] N. Sun, J. Wang, J. Yao, C. Deng, Anal. Chem. 89 (2017) 1764–1771.
[41] X. Xu, C. Deng, M. Gao, et al., Adv. Mater. 18 (2006) 3289–3293.
[42] L. Li, Y. Qiu, J. Huang, et al., Water Air Soil Poll. 225 (2014) 2220.
[43] R. Eivazzadeh-Keihan, H. Bahreinizad, Z. Amiri, et al., TrAC: Trend. Anal. Chem. 141 (2021) 116291.
[44] W. Zhang, M. Lin, M. Wang, et al., J. Chromatogr. A 1503 (2017) 1–11.
[45] A. Bajracharya, Y.L. Liu, J.J. Lenhart, Env. Sci Water Res. Technol. 5 (2019) 256–267.
[46] K. Zhou, J. Wu, H. Liu, Environ. Pollut. 271 (2021) 116320.
[47] A. Sinha, N.R. Jana, ACS Appl. Mater. Interfaces 7 (2015) 9911–9919.
[48] C. Huang, Y. Wang, Q. Huang, Y. He, L. Zhang, Anal. Chim. Acta 1054 (2019) 38–46.
[49] X.Y. Liu, S.Q. Gao, X.Y. Li, et al., Ecotoxicol. Environ. Saf. 176 (2019) 20–26.
[50] Q.Y. Li, L.L. Lian, X.Y. Wang, et al., J. Separ. Sci. 40 (2017) 1644–1650.